A cylindrical cavity expansion test on sand

Shay Nachum[1], *Mark* Talesnick[2], and *Mason* Ghafghazi[1#]

[1]*University of Toronto, Civil & Mineral Engineering, 35 St. George St. Toronto, ON, Canada*
[2]*Technion – Israel Institute of Technology, Civil & Environmental Engineering, Haifa 32000, Israel*
[#]*Corresponding author: mason.ghafghazi@utoronto.ca*

ABSTRACT

Cylindrical cavity expansion is one of the fundamental boundary value problems in geotechnical engineering used as a simplified analogue to the pressuremeter test, pile driving and the Cone Penetration Test. Much of the popularity of cavity expansion comes from the simplicity of modelling it numerically. All numerical models require verification and validation, but doing so for cavity expansion has been limited due the relatively small amount of physical modelling of the problem. Past cavity expansion tests in calibration chambers have often been limited in range of strains, diameter to length ratio, and the amount and type of measurements made.
This paper describes a calibration chamber set up used to perform cylindrical cavity expansion tests in a dry fine sand. Instead of attempting to replicate a specific application (e.g., pressuremeter test), the goal was to create a near-perfect cylindrical cavity expansion model, with in-soil measurement of stresses and strains, to serve as baseline data for validation of numerical models. The experimental set up is described, the material properties are summarized, and results of a cavity expansion tests are presented and discussed.

Keywords: cavity expansion; pressuremeter; monitoring techniques.

1. Introduction

Cavity expansion is a fundamental boundary value problem that is seen as an analogue to many geotechnical engineering applications, such as anchor uplift resistance (Lee et al., 2012; Zhuang and Yu, 2018), simulate pre-split blasting mechanism in the mining industry (Wang et al., 2013), pile driving (Li et al., 2017; Burali d'Arezzo et al., 2015), and tunnelling (Vrakas and Anagnostou, 2014; Liu et al., 2020). One of the main applications of cavity expansion is the interpretation of pressuremeter and cone penetration tests (e.g. Mayne, 1991; Chang et al., 2001; Cudmani and Osinov, 2001; Shuttle, 2006; Ghafghazi and Shuttle, 2008; Mo et al., 2017).

While modelling cavity expansion numerically has been popular due to its simplicity, there are only a few attempts at physical modelling. Such physical models can be used for validating numerical approaches, direct comparisons to the proxy problems, or further understanding soil behaviour under different loading conditions.

Zimberlin et al. (2007) examined spherical cavity expansion by injecting a pressurized fluid at the tip of a needle embedded in a gel, in order to quantify the mechanical properties of naturally heterogeneous materials. Raayai-Ardakani et al. (2019) followed a similar approach and compared the results to numerical simulations, in order to characterize the local stiffening response and quantify shear modulus. Nafo and Al-Mayah (2019) did similar work using a catheter.

In geomechanics, Wang et al. (2010a,b) examined spherical cavity expansion in soils in a triaxial setup by injecting water through a needle to expand a balloon, which caused compaction of the surrounding soil. Their purpose was to investigate the compaction grouting process. The compaction process is considered as a cavity expansion process in the numerical simulations. They investigated the relation between the injection pressure, void ratio and excess pore water pressure at various radial distances from the injection point. The pressure-controlled cavity expansion laboratory tests were carried out to validate the finite element analyses.

The pressuremeter test is a particular case of cylindrical cavity expansion with a limited length to diameter ratio. The pressuremeter test is an in-situ stress-strain test performed on the wall of a borehole using a cylindrical probe that is expanded radially. (e.g. Ajalloeian and Yu, 1998; ASTM, 2000). To obtain viable test results, disturbance between the pressuremeter and the soil must be minimized. Bellotti et al. (1989) performed a wished-in installations in a controlled laboratory environment where sand was pulvinated in place around a pressuremeter. This installation procedure was adopted in the current work.

Laboratory-scale pressuremeter tests have been performed previously by several researchers (e.g. Nasr and Gangopadhyay, 1988; Tan, 2005; Thorel et al., 2007; Johnston et al., 2013), and shown to be efficient and reliable.

This paper reports results from a cylindrical cavity expansion test. A high length to diameter ratio was created and three normal strains and stresses were measured at a point near the cavity. The experimental set up is described, the material properties are summarized, and results of the test are discussed.

2. Material

The sand tested is a fine, uniformly graded, 85-90% quartz (Sandler et al. 2023) sand from Caesarea, Israel, referred to as dune sand. The mean grain size (D_{50}) is 0.28 mm, coefficient of uniformity, c_u =1.7 and coefficient of curvature, c_c = 0.9. The specific gravity of particles, *Gs*, is 2.67. The maximum and minimum void ratios e_{max} and e_{min} are 0.93 and 0.55, respectively.

The critical state parameters of the dune sand (Table 1) were classified by 15 triaxial compression tests. The tests were performed on 50 mm diameter and 102 mm tall specimens. The triaxial testing were performed according to procedures outlines by Manmatharajan et al. (2023). Two preparation methods were used: air-pluviation - AP (from different heights) and moist tamping - MT.

Table 1. Critical State parameters of dune sand

Parameter	Value	Remarks
Γ	0.858	"altitude" of CSL, defined at 1 kPa
λ	0.061	slope of CSL, defined on base 10
M	1.25	stress ratio q/p' at the critical state

3. Testing procedure

The test was performed in a cylindrical chamber with walls acting as rigid boundaries. The inner diameter of the chamber is 750 *mm*, and wall height is 510 *mm*. In the centre, the height of the chamber is a maximum of 640 *mm*. The tank volume is 0.253 m^3. Two layers of polyethylene sheets lubricated with graphite grease in between were placed on the inner walls to reduce wall friction.

The specimen was prepared by carefully funnelling dry sand into the chamber from a height of 10-30 *mm*. The nominal void ratio obtained from air pluviation was 0.722, before being consolidated to 0.684 under 100 *kPa*. At this void ratio, the relative density is 65% and the state parameter is -0.064.

The chamber was filled to the chosen height, at which point pluviation was haulted to place the in-soil measurement sensors at a 33 *mm* distance from the central axis of the cavity, in the vertical, radial, and circumferential directions. These three directions describe the full stress and strain tensor, assuming plane strain conditions in the mid-height of the cavity.

After installing sensors, the chamber was filled to the top. The specimen top surface was levelled, and a latex membrane was placed between the sand top surface and the tank lid. 100 *kPa* air pressure was applied through the lid into the void between the lid and the membrane. The test was performed on sand in the normally consolidated (compressed) state.

The cavity was created by expanding a latex tube sealed around a central pipe 7 *mm* in diameter and 400 mm long (Fig. 1a). Two floating 40 *mm* OD Teflon donuts were placed at both ends of the rod to confine the expanding tube to a cylindrical shape. The starting length to diameter ratio was 57; the highest among existing experiments. During cavity expansion, the pressure inside the latex tube was gradually increased. In the experiment described in this paper, the cavity volume was not successfully monitored, hence the cavity radius

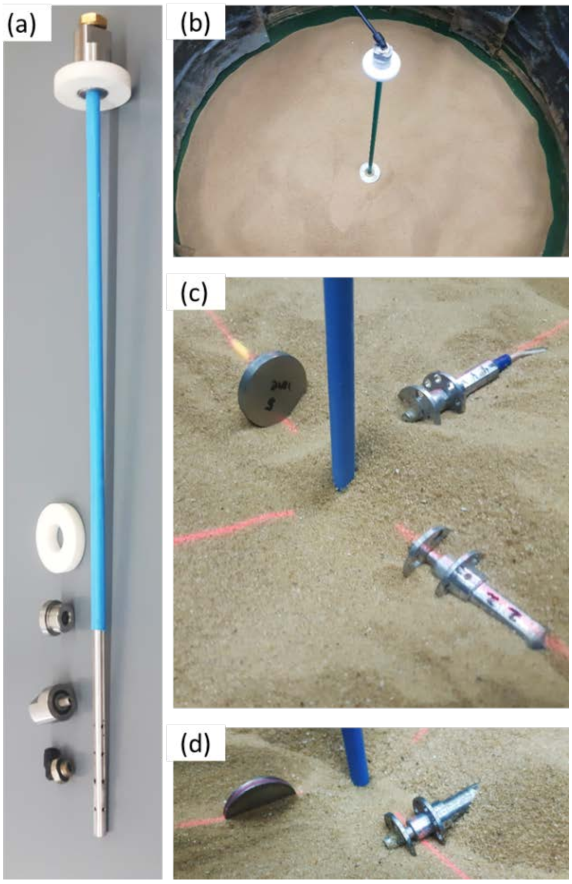

Figure 1. Test setup: (a) cavity tube and membrane; (b) cavity set up before specimen preparation; (c) view of in-soil pressure sensor to measure σ_r and in-soil strain sensor to measure ε_r; (d) sensors orientation for measure σ_θ and ε_θ

in the expansion is unknown. This is being rectified for future tests.

3.1. In-soil measurements

Normal stresses in the vertical, radial, and circumferential directions were measured using Null Soil Pressure Gauges (Talesnick, 2005). Null sensors are based on maintaining zero diaphragm deflection through a servo-controlled air pressure system (Fig. 1c and 1d). Talesnick et al. (2014) and Talesnick and Bolton (2020) showed that by eliminating diaphragm deflection more accurate and representative normal soil pressures are registered. The gauges employed had an overall diameter of 25 mm, a sensing diameter of 13 mm, and a nominal diaphragm thickness of 0.3 mm.

In-soil normal strains were measured using an LVDT (linear variable displacement transducer) based sensor (Fig. 1c and 1d). The normal strain sensor housing is composed of two telescopic tubes: one holds the LVDT body and the other holds the magnetic core. Each of the two tubes are capped by a disc which forces the housing to move together with the surrounding soil. Normal strain was calculated by dividing the relative deformation measured over the sensor length by the initial distance between the discs. More details and examples of application of these sensors can be found in Talesnick and Bolton (2020) and Talesnick and Omer (2023).

4. Results

At the end of consolidation to 100 *kPa* vertical stress, the three null pressure gauges registered 42 *kPa*, 46 *kPa*, and 100 *kPa* in, the radial circumferential, and vertical directions, resulting in a K_0 value estimated to be 0.44.

Figure 2 shows the pressure applied in the cavity as a function of time. Pressure was increased, upon reaching a cavity pressure of 330 *kPa*, the pressure was reduced to 50 *kPa*, and then reloaded to an internal pressure of 360 *kPa* at which time the latex tube burst.

Figure 3 shows the stresses measured 33 *mm* from the cavity center as functions of cavity pressure. The results illustrate that as the cavity pressure increases, the radial stress increases, and the circumferential and vertical stresses decrease.

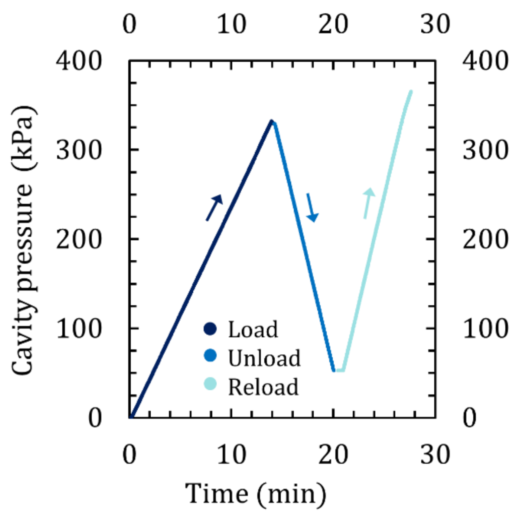

Figure 2. Cavity pressure as a function of time

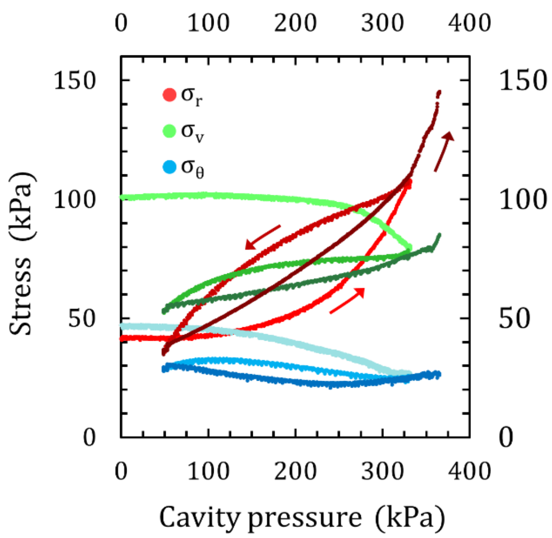

Figure 3. Radial, vertical and circumferential stresses, 33 mm from the cavity center, as functions of cavity pressure

Figure 4 shows the strains measured 33 mm from the cavity center as functions of the cavity pressure. With the cavity expansion, the radial strain increased as expected. The vertical strain slightly increased in compression. The minuscule change in the vertical strain confirms practically plane strain conditions at the middle of the expanding cylinder. The circumferential strain registered was negative, implying expansion in that direction. The unload-reload cycles in both stress and strain show hysteresis as expected.

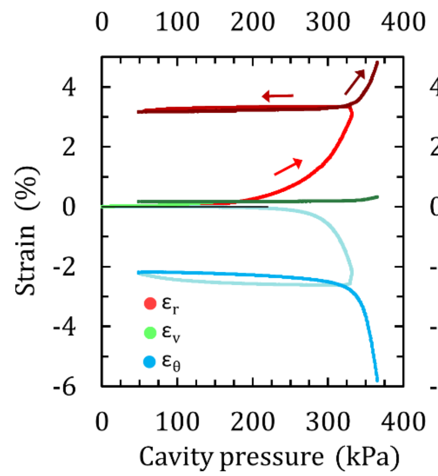

Figure 4. Radial, vertical and circumferential strains, 33 mm from the cavity center.

Figure 5 shows the volumetric strain computed from the three measured strains, suggesting contractive, followed by dilative behaviour 33 *mm* away from the cavity.

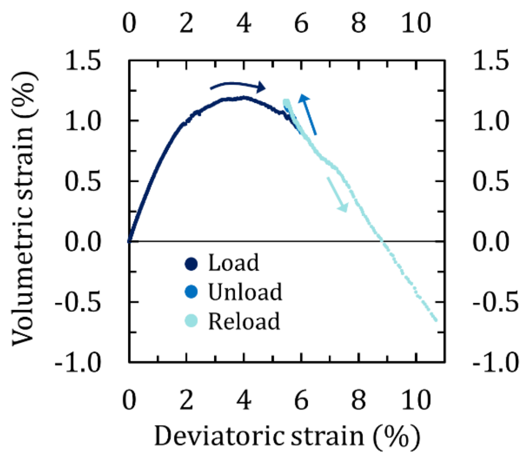

Figure 5. Volumetric strain as a function of deviator strain, 33 mm from the cavity center

Combining Figures 3 and 4, it is possible to plot the radial, circumferential and vertical stresses as functions of their corresponding strains, as shown in figure 6.

The vertical strains in Figure 6 are so small a clear trend was not observed. The radial stress-strain curve resemble load-unload-reload behaviour, with a stiff unload-reload behaviour. The circumferential stress-strain curve shows a similar trend, albeit in the negative direction, with expansion of strains, and reduction of stresses.

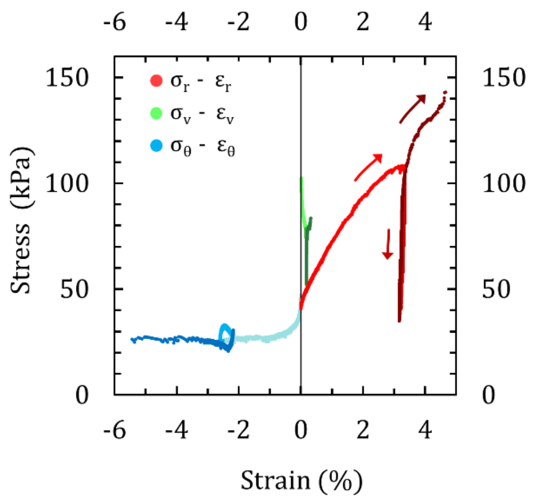

Figure 6. Radial, vertical and circumferential stress-strain curves, 33 mm from the cavity center

Combining measured stresses to compute the mean effective stress p' and deviator stress q as functions of the cavity pressure in Figure 7. The trends are somewhat similar. Both p' and q start fairly soft and increase more rapidly at higher cavity pressures. The unload-reload cycle has the typical hysteresis shape for both p' and q.

Figure 8 shows the stress path in the $p' - q$ plot. The stress state starts at a stress ratio of $q/p' = 0.89$ and shows a drop before rising on a 4 to 1 loading path. The unloading more or less follows the same 4 to 1 path before turning towards the origin. Upon reloading a 2 to 1 path takes the stress state towards the starting point and the earlier loading path and passes those along the same 2 to 1 path. The path appears to be approaching the critical state line as the test ended.

A comparison between the vertical strain and stress in figures 3 and 4 suggest that the loading in the middle section of the cavity/chamber is much closer to plain-strain than it is to plane-stress.

Figure 5 indicates that the volumetric strain in the later stages of the test is dilative. Allthough the test is a cavity expansion, and therefore the soil in general expected to be compressed. At a distance of 33 mm from the cavity center, for this specimen at 65% relative density, dilation was strong enough to eventually overcome compression.

5. Conclusions

A calibration chamber set up was developed for cylindrical cavity expansion testing in dry sand. A cavity expansion test was described, and stresses and strains near the cavity were measured. It was demonstrated that in the middle section of the cavity, near plane strain conditions prevail. Radial stresses and strains follow the expected trend, with a stiff unload-reload. Circumferential stresses and strains showed expansion conditions as expected as the radius increased.
The volumetric strains computed from the three normal strains measured showed that the dilative tendencies of the medium dense specimen overcame the general compressive regime imposed by the expanding cavity at 33 mm distance from the cavity.

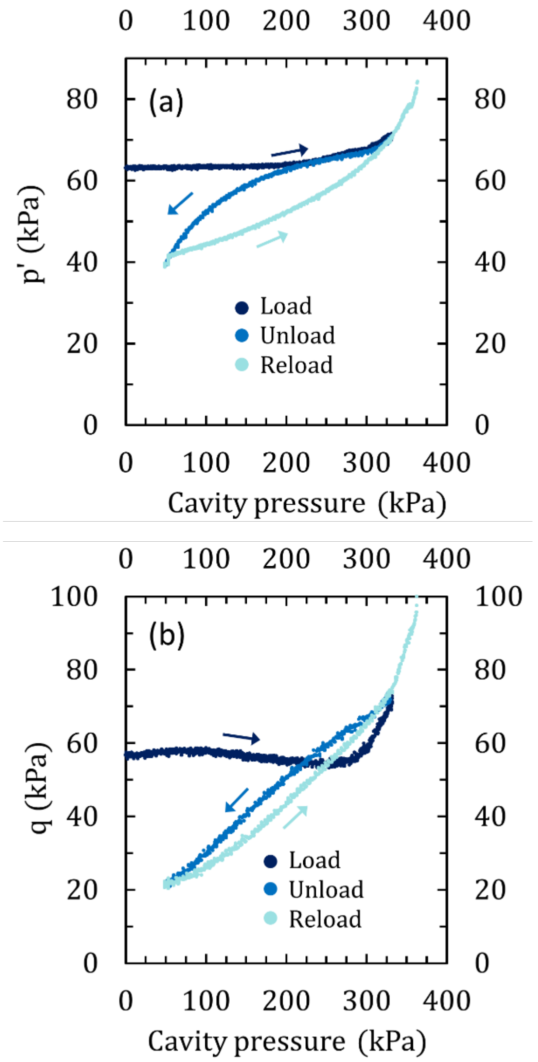

Figure 7. Stress invariants as functions of cavity pressure; a) mean stress, p', and; b) deviator stress, q

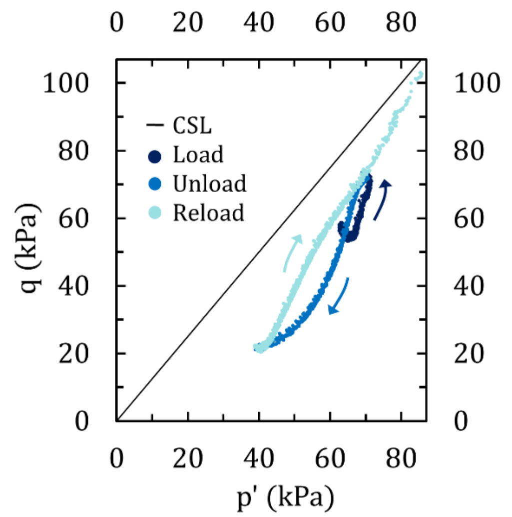

Figure 8. Stress paths in the $p' - q$ plane

The mean and deviator stresses computed from the three normal stresses showed that the stress path at 33 mm distance follows a reasonable trend and appears to be approaching the critical state when the test was terminated.

Future work will include other specimen densities, higher pressures, measurements of stresses and strains at more distances from the cavity, an assessment of potential boundary effects, and most importantly, accurate measurement of cavity radius as the pressure increases.

References

Ajalloeian, R., and Yu, H. S. 1998. “Chamber studies of the effects of pressuremeter geometry on test results in sand.” Geotechnique, 48(5), 621-636.

ASTM, D.4719-00. 2000 “Standard test method for prebored pressuremeter testing in soils”. American Society for Testing & Materials Standard.

Burali d’Arezzo, F., Haigh, S., Talesnick, M., and Ishihara, Y. 2015. "Measuring horizontal stresses during jacked pile installation." Proceedings of the Institution of Civil Engineers-Geotechnical Engineering, 168(4), 306-318.

Bellotti, R., Ghionna, V., Jamiolkowski, M., Robertson, P. K., and Peterson, R. W. 1989. “Interpretation of moduli from self-boring pressuremeter tests in sand.” Géotechnique, 39(2), 269-292.

Chang, M.F., Teh, C.I., and Cao, L.F. 2001. “Undrained cavity expansion in modified Cam clay II: Application to the interpretation of the piezocone test.” Géotechnique 51 (4), 335–350. https://doi.org/10.1680/geot.2001.51.4.335.

Cudmani, R., and Osinov, V.A. 2001. “The cavity expansion problem for the interpretation of cone penetration and pressuremeter tests”. Can. Geotech. J. 38 (3), 622–638.

Ghafghazi, M., and Shuttle, D. 2008. “Interpretation of sand state from cone penetration resistance.” Géotechnique, 58(8), 623-634.

Johnston, G., Doherty, J., and Lehane, B. 2013. “Development of a laboratory-scale pressuremeter.” International Journal of Physical Modelling in Geotechnics, 13(1), 31-37.

Li, J.P., Gong, W.B., Li, L., and Liu, F. 2017. “Drained elastoplastic solution for cylindrical cavity expansion in K0-consolidated anisotropic soil.” J. Eng. Mech. 143 (11).

Liu, K., Chen, S.L., and Gu, X.Q. 2020. “Analytical and numerical analyses of tunnel excavation problem using an extended Drucker-Prager model.” Rock Mech. Rock Eng. 53 (4), 1777–1790. https://doi.org/10.1007/s00603-019-01992-5.

Mayne, P.W. 1991. “Determination of OCR in clays by piezocone tests using cavity expansion and critical state concepts. Soils Found.” 31 (2), 65–76. https://doi.org/10.3208/sandf1972.31.2_65.

Manmatharajan, M. V., Gill, S., Liu, W., Ingabire, E. P., Sy, A., and Ghafghazi, M. 2023. “Effect of Particle Size and Particle Size Distribution on Critical State Loci of Granular Soils.” Canadian Geotechnical Journal.

Mo, P.Q., Marshall, A.M., and Yu, H.S. 2017. “Interpretation of cone penetration test data in layered soils using cavity expansion analysis.” J. Geotech. Geoenviron. Eng. 143 (1), 04016084. https://doi.org/10.1061/(ASCE)GT.1943-5606.0001577.

Nafo, W., and Al-Mayah, A. 2019. “Measuring hyperelastic properties of hydrogels using cavity expansion method.” Experimental Mechanics, 59(7), 1047-1061.

Nasr, A. N., and Gangopadhyay, C. R. 1988. “Study of Su predicted by pressuremeter test.” Journal of Geotechnical Engineering, 114(11), 1209-1226.

Raayai-Ardakani, S., Chen, Z., Earl, D. R., and Cohen, T. 2019. “Volume-controlled cavity expansion for probing of local elastic properties in soft materials.” Soft matter, 15(3), 381-392.

Sandler, A., Taitel-Goldman, N., and Ezersky, V. 2023. “Sources and formation of iron minerals in eastern Mediterranean coastal sandy soils–A HRTEM and clay mineral study.” Catena, 220, 106644.

Shuttle, D. A. 2006. “Can the effect of sand fabric on plastic hardening be determined using a self-bored pressuremeter?” Canadian geotechnical journal, 43(7), 659-673.

Talesnick, M. 2005. “Measuring soil contact pressure on a solid boundary and quantifying soil arching.” Geotech. Test. J. 28 (2), 12484. https://doi.org/10.1520/GTJ12484.

Talesnick, M.L., Ringel, M., and Avraham, R. 2014. “Measurement of contact soil pressure in physical modelling of soil–structure interaction.” Int. J. Phys. Model. Geotech. 14 (1), 3–12.

Talesnick, M.L., and Bolton, M.D. 2020. “Effect of structural boundaries and stress history on at-rest soil pressure of sand.” Int. J. Phys. Model. Geotech. 1–10.

Talesnick, M., and Omer, I. 2023. “Measurement of stresses and strains around a pushed in model pile or cone penetrometer.” International Journal of Physical Modelling in Geotechnics, 1-26.

Tan, N. K. 2005. “Pressuremeter and cone penetrometer testing in a calibration chamber with unsaturated Minco silt.” Ph.D. thesis, University of Oklahoma, Norman, Okla.

Thorel, L., Gaudin, C., Rault, G., Garnier, J., and Favraud, C. 2007. “A cone pressuremeter for soil characterisation in the centrifuge.” International Journal of Physical Modelling in Geotechnics, 7(1), 25-32.

Vrakas, A., Anagnostou, G. 2014. “Finite strain elastoplastic solutions for the undrained ground response curve in tunnelling”. Int. J. Numer. Anal. Meth. Geomech. 39 (7), 738–761. https://doi.org/10.1002/nag.2335.

Wang, S. Y., Chan, D. H., Lam, K. C., and Au, S. K. A. 2010a. “Effect of lateral earth pressure coefficient on pressure controlled compaction grouting in triaxial condition.” Soils and foundations, 50(3), 441-445.

Wang, S. Y., Chan, D. H., Lam, K. C., and Au, S. K. A. 2010b. “Numerical and experimental studies of pressure-controlled cavity expansion in completely decomposed granite soils of Hong Kong.” Computers and Geotechnics, 37(7-8), 977-990.

Wang, F., Tu, S., Yuan, Y., Feng, Y., Chen, F., and Tu, H., 2013. “Deep-hole pre-split blasting mechanism and its application for controlled roof caving in shallow depth seams.” Int. J. Rock Mech. Min. Sci. 64, 112–121. https://doi.org/10.1016/j.ijrmms.2013.08.026.

Zhuang, P.Z., and Yu, H.S., 2018. “Uplift resistance of horizontal strip anchors in sand: a cavity expansion approach.” Géotech. Lett. 8 (4), 284–289.
https://doi.org/10.1680/jgele.18.00083.

Zimberlin, J. A., Sanabria-DeLong, N., Tew, G. N., and Crosby, A. J. 2007. “Cavitation rheology for soft materials.” Soft Matter, 3(6), 763-767.